ARL-RP-0556 • OCT 2015

US Army Research Laboratory

Comparison of JP-8 Sprays from a Hydraulically Actuated Electronically Controlled Unit Injector and a Common Rail Injector

by Matthew Kurman, Michael Tess, Luis Bravo, Chol-Bum Kweon, and Craig Hershey

Reprinted from ILASS Americas [accessed 2015 Sep 16]. http://www.ilass.org/2/recent-papers-form.html. Paper presented at ILASS Americas 27th Annual Conference on Liquid Atomization and Spray Systems; 2015 May 17–20; Raleigh, NC.

NOTICES

Disclaimers

ARL-RP-0556 ● OCT 2015

US Army Research Laboratory

Comparison of JP-8 Sprays from a Hydraulically Actuated Electronically Controlled Unit Injector and a Common Rail Injector

by Matthew Kurman, Michael Tess, Luis Bravo, and Chol-Bum Kweon
Vehicle Technology Directorate, ARL

Craig Hershey
US Army Materiel Systems Analysis Activity, Aberdeen Proving Ground, MD

Reprinted from ILASS Americas [accessed 2015 Sep 16]. http://www.ilass.org/2/recent-papers-form.html. Paper presented at ILASS Americas 27th Annual Conference on Liquid Atomization and Spray Systems; 2015 May 17–20; Raleigh, NC.

REPORT DOCUMENTATION PAGE

Form Approved
OMB No. 0704-0188

1. REPORT DATE *(DD-MM-YYYY)*
October 2015

2. REPORT TYPE
Reprint

3. DATES COVERED (From - To)
January 2015–March 2015

4. TITLE AND SUBTITLE
Comparison of JP-8 Sprays from a Hydraulically Actuated Electronically Controlled Unit Injector and a Common Rail Injector

5a. CONTRACT NUMBER

5b. GRANT NUMBER

5c. PROGRAM ELEMENT NUMBER

6. AUTHOR(S)
Matthew Kurman, Michael Tess, Luis Bravo, Chol-Bum Kweon, and Craig Hershey

5d. PROJECT NUMBER

5e. TASK NUMBER

5f. WORK UNIT NUMBER

7. PERFORMING ORGANIZATION NAME(S) AND ADDRESS(ES)
US Army Research Laboratory
ATTN: RDRL-VTP
Aberdeen Proving Ground, MD 21005-5066

8. PERFORMING ORGANIZATION REPORT NUMBER
ARL-RP-0556

9. SPONSORING/MONITORING AGENCY NAME(S) AND ADDRESS(ES)

10. SPONSOR/MONITOR'S ACRONYM(S)

11. SPONSOR/MONITOR'S REPORT NUMBER(S)

12. DISTRIBUTION/AVAILABILITY STATEMENT
Approved for public release; distribution is unlimited.

13. SUPPLEMENTARY NOTES
Reprinted from ILASS Americas [accessed 2015 Sep 16]. http://www.ilass.org/2/recent-papers-form.html. Paper presented at ILASS Americas 27th Annual Conference on Liquid Atomization and Spray Systems. 2015 May 17–20; Raleigh, NC.

14. ABSTRACT
JP-8 sprays from a hydraulically actuated electronically controlled unit injector (HEUI) and a common rail injector (CRIN) were investigated to compare the effects of the fuel delivery system on the spray behavior of the fuel. The fuel pressurization method between injectors is fundamentally different. The HEUI system utilizes engine oil to pressurize the fuel, whereas, the CRIN system pressurizes the fuel directly. To explore the different injection methods, rate of injection (ROI) experiments were initially conducted to measure shot-to-shot fuel quantity and rate of injection of both injector types. During the ROI experiments with the HEUI, the oil temperature and pressure was varied from 45°C to 90°C and 142-200 bar, respectively. In addition, the dwell time and rate shape of the HEUI was investigated to determine effects on injected fuel mass and rate of injection. Non-reacting spray experiments were performed in a high temperature (900 K), high pressure (60 bar) flow chamber to investigate the transient liquid penetration lengths of both injection systems. Ambient conditions of the flow chamber were chosen to represent typical conditions found in a compression-ignition engine and fuel injection pressures were 850, 1000, and 1200 bar. Results showed that an increase in oil temperature for the HEUI will increase the injected fuel mass. The CRIN injector system showed 4 times more precise control of injected fuel mass compared to the HEUI, and the CRIN showed less variations in the hydraulic delay. Comparing the plume to plume transient spray behavior of the two systems showed that more variations were present with the HEUI injector. However, the overall transient liquid penetration behavior was similar for both injection systems. Results of this study can be used to optimize the design of engines using JP-8 with hydraulic fuel injectors, thus improving fuel efficiency and power output.

15. SUBJECT TERMS
HEUI, JP-8, injector, spray, CRIN

16. SECURITY CLASSIFICATION OF:			17. LIMITATION OF ABSTRACT	18. NUMBER OF PAGES	19a. NAME OF RESPONSIBLE PERSON
					Matthew Kurman
a. REPORT	b. ABSTRACT	c. THIS PAGE			19b. TELEPHONE NUMBER (Include area code)
Unclassified	Unclassified	Unclassified	UU	22	410-278-8971

Standard Form 298 (Rev. 8/98)
Prescribed by ANSI Std. Z39.18

Comparison of JP-8 Sprays from a Hydraulically Actuated Electronically Controlled Unit Injector and a Common Rail Injector

Matthew Kurman*, Michael Tess, Luis Bravo, and Chol-Bum Kweon
U.S. Army Research Laboratory, Aberdeen Proving Ground, MD 21005
&
Craig Hershey
U.S. Army Materiel Systems Analysis Activity, Aberdeen Proving Ground, MD 21005

Abstract

JP-8 sprays from a hydraulically actuated electronically controlled unit injector (HEUI) and a common rail injector (CRIN) were investigated to compare the effects of the fuel delivery system on the spray behavior of the fuel. The fuel pressurization method between injectors is fundamentally different. The HEUI system utilizes engine oil to pressurize the fuel, whereas, the CRIN system pressurizes the fuel directly. To explore the different injection methods, rate of injection (ROI) experiments were initially conducted to measure shot-to-shot fuel quantity and rate of injection of both injector types. During the ROI experiments with the HEUI, the oil temperature and pressure was varied from 45°C to 90°C and 142-200 bar, respectively. In addition, the dwell time and rate shape of the HEUI was investigated to determine effects on injected fuel mass and rate of injection. Non-reacting spray experiments were performed in a high temperature (900 K), high pressure (60 bar) flow chamber to investigate the transient liquid penetration lengths of both injection systems. Ambient conditions of the flow chamber were chosen to represent typical conditions found in a compression-ignition engine and fuel injection pressures were 850, 1000, and 1200 bar. Results showed that an increase in oil temperature for the HEUI will increase the injected fuel mass. The CRIN injector system showed 4 times more precise control of injected fuel mass compared to the HEUI, and the CRIN showed less variations in the hydraulic delay. Comparing the plume to plume transient spray behavior of the two systems showed that more variations were present with the HEUI injector. However, the overall transient liquid penetration behavior was similar for both injection systems. Results of this study can be used to optimize the design of engines using JP-8 with hydraulic fuel injectors, thus improving fuel efficiency and power output.

*Corresponding author: matthew.s.kurman.civ@mail.mil

Introduction

To fully optimize the fuel efficiency and power output of internal combustion engines and to reduce harmful emissions, it is essential to understand the complex physical and chemical processes occurring during fuel injection events. Proper fuel delivery will enable fuel atomization to occur and lead to optimized fuel/air mixing for combustion. Characterizing fundamental spray behavior such as rate of injection (ROI) and transient liquid penetration length is essential for the advancement and development of current and next generation engine designs.

Fuel delivery systems such as the hydraulically actuated electronically controlled unit injector (HEUI) and the common rail (CRIN) fuel injector precisely control the delivery of fuel to the engine. However, each system is fundamentally different in regards to the method used to pressurize the fuel. The HEUI system utilizes the oil from the engine to pressurize the fuel for injection. The engine oil passes to an intensifier piston and plunger inside the injector which acts on the low pressure fuel to amplify the fuel pressure independent from engine speed [1, 2]. Once the fuel is pressurized, an electronically controlled poppet valve is triggered for injection. The common rail injection system directly pressurizes the fuel to the desired injection pressure. Fuel is supplied to a high pressure pump where the fuel is compressed to increase the pressure. The high pressure fuel is then directed to a common rail and ultimately to the fuel injector where an electronically controlled solenoid engages a control valve which allows fuel to flow from the injector. A more thorough description of the HEUI and common rail systems can be found elsewhere [3].

Previous research on comparing HEUI and common rail injection has been reported. Experiments with a spray chamber and engine were conducted to analyze liquid penetration length and emissions from both fuel injection systems [4]. Results from the study showed that the rate of injection between each system affects the overall emissions from combustion. In another study, injection rate meter experiments were performed to characterize the different injection systems [3]. Results from the study were used to validate CFD predictions for highlighting effects of injector design parameters, such as outlet to inlet throttle ratios of the fuel passage inside the injector. Furthermore, a comparison of liquid penetration lengths was conducted to explore the effect of rate of injection and injection pressure between injection systems [5]. Results showed that there were negligible effects on penetration length from varying injection pressure and rate of injection. In addition, X-ray radiography was used to describe spray behavior of HEUI and common rail injectors and results showed that the HEUI provided a broader spray based on mass distribution. [6].

However, the studies mentioned investigated diesel or a diesel reference fuel. Power generating systems for military applications are mandated to use JP-8 fuel through DoD Directive 4140.43. In the present study, JP-8 sprays from a HEUI and common rail CRIN fuel injector were initially characterized with a fuel rate of injection instrument and then in a constant pressure flow chamber. The common rail injector was characterized to provide baseline parameters and the rate of injection profile for the HEUI was tuned to match the behavior. HEUI rate of injection tuning was also conducted in a study investigating size scaling parameters [7]. Similar rate of injection profiles, injected fuel mass, and Reynolds/Weber numbers were determined for both injection systems. To further investigate the different injection systems, non-reacting JP-8 sprays from the injectors were also examined in a high temperature (900 K), high pressure (60 bar) environment to compare transient characteristics of the liquid fuel sprays.

Experimental Setup

Injection Characterization

To characterize the rate of injection and injected fuel mass, fuel injection experiments for both the HEUI and the CRIN were conducted with an IAV injection analyzer. The injection analyzer is a Bosch style instrument that operates on the relationship that the injected fuel mass is proportional to the speed of sound in the fuel [8]. During the ROI experiments, 100 shot averages of both injected fuel mass and rate of injection were acquired. To enable a direct comparison of spray characteristics between injector systems in the constant pressure flow chamber, the Reynolds and Weber numbers and injected fuel mass were held constant between each injector. As a baseline, the CRIN injector was mapped for a constant energizing time of 470 us for the fuel pressures of 850, 1000, and 1200 bar. During injector mapping of the HEUI, the pilot and dwell times were adjusted to yield a corresponding rate shape that matched the rate shape of the CRIN injector. The dwell time is defined as the time between the end of the commanded pilot injection and the start of the commanded main injection. By keeping the fuel pressure, rate shapes, and the overall injected fuel mass similar, rate of injection and Reynolds/Weber numbers can be held constant between injection systems. Table 1 shows Reynolds and Weber numbers for an estimated fuel temperature of 358 K for the fuel injection pressures investigated. Both the CRIN and the HEUI fuel injectors were controlled by a Drivven direct injector driver system. Figure 1 shows the current profile used for the CRIN injector for all experiments. The example profile for the HEUI in Figure 1 consists of a 554 us pilot, 900 us dwell, and 480 us main energizing time and these parameters were varied depending on the experiment being conducted.

Table 1. Re and We Numbers.

Fuel Pressure [bar]	Re [x 10^4]	We [x 10^6]
850	8.3	1.3
1000	9.0	1.6
1200	9.9	1.9

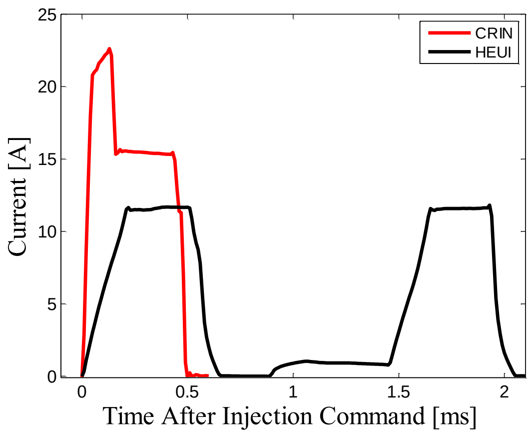

Figure 1. Current profiles of both the HEUI and CRIN injector.

Constant Pressure Flow Chamber

Non-reacting JP-8 spray experiments were conducted in a stainless-steel high temperature constant pressure flow chamber. The chamber was designed to provide a well defined temperature/pressure ambient environment. A schematic of the flow chamber and experimental setup is shown in Figure 2. For the non-reacting experiments discussed in this study, the ambient gas composition consisted of 100 % nitrogen, and the ambient temperature and pressure were maintained at 900 K and 60 bar, respectively with a corresponding ambient density of 22.5 kg/m^3. The temperature and pressure were chosen to represent realistic typical conditions found in a compression ignition engine near the start of fuel injection. Nitrogen is supplied by an onsite nitrogen generator and is compressed by a high pressure compressor. Heating of the ambient gas is supplied by 2 cartridge heaters and a ceramic style heater in the testing section. The flow rate through the chamber is maintained at 58 m^3/hr during experiments. Optical access is provided by 3, 147 mm diameter and 85 mm thick, UV grade fused silica windows.

Fuel Injection Systems

Since the CRIN and HEUI fuel injectors pressurize fuel in different ways, two fuel pressurization systems were used during the experiments for this study. The common rail fuel injection system consists of an air driven pump capable of directly pressurizing the fuel by using compressed air. In this system, fuel pressure is controlled by adjusting the supplied compressed air. The pressurized fuel is then directed to a common rail, and the fuel is sent to the CRIN fuel injector. A CRIN fuel injector mount holds the fuel injector to the pressure chamber during experiments.

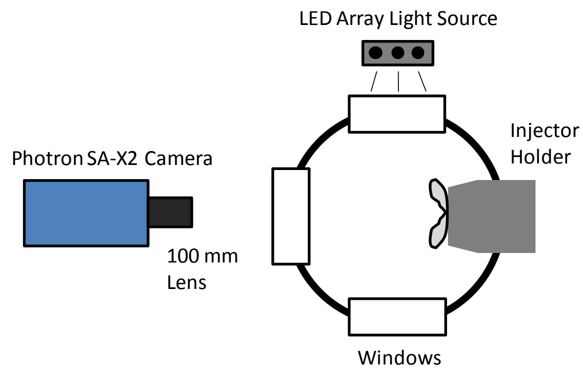

Figure 2. Schematic of the Mie scattering optical setup with the high temperature constant pressure flow chamber.

As mentioned, the HEUI fuel injector relies on the oil pressurization system of an engine to pressurize the fuel. In a HEUI injector, the internal hydraulic intensifier system provides an amplification factor to supply the high pressure for fuel injection. The amplification ratio for the injector used in this study was 6 to 1, which corresponds to the fuel injection pressure being a factor of 6 larger than the supplied oil pressure. In addition, the rate shape of the HEUI injector can depend on a pilot injection which acts as a primer for the main injection. The pilot injection is separated from the main injection event by a dwell time. By adjusting the pilot and dwell time, the overall rate shape of the injection event can be tuned. Various rate shapes are achievable and can alter engine performance and emissions [9]. A photograph of the fuel injectors are shown in Figure 3.

To utilize the HEUI fuel injector isolated from an engine, a fuel bench was designed to supply both fuel and high pressure oil to the injector. The fuel bench consists of a 5 hp electric motor that drives a high pressure oil pump, and a low pressure gear pump for pressurizing the fuel supply. The oil pump is capable of pressurizing the oil up to 200 bar and the low pressure fuel supply pump is capable of pressures up to 7 bar. To condition the oil and fuel by simulating temperature conditions commonly found with an actual engine, the fuel bench is also equipped with immersion heaters and cooling water heat exchangers that allow temperature control of the liquids.

Figure 3. Photograph of the HEUI (left) and CRIN (right) fuel injectors.

Unlike the CRIN injector which only requires a fuel supply and a solid fixture to mount the injector to the flow chamber, the HEUI injector also requires a supply of high pressure, high temperature oil. Therefore, a stainless steel HEUI injector mounting fixture, as shown in Figure 4, was designed with internal oil and fuel passages to allow for mounting the injector to the chamber. For the experiments presented in this study, 3 fuel pressures were investigated, 850, 1000, and 1200 bar.

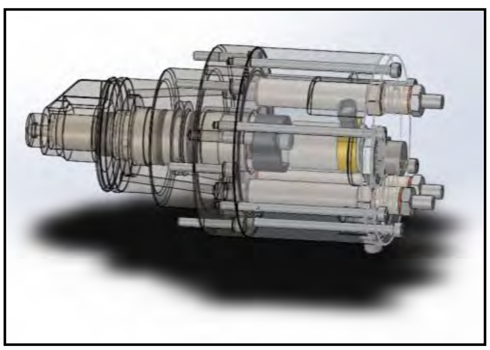

Figure 4. Model of the HEUI injector holder showing internal flow passages for oil and fuel.

To determine the actual orifice diameters of each of the 6 orifices on each injector, an Olympus SZH10 optical microscope was used. Prior to measuring the orifices, images where acquired of a calibration plate to provide scaling for the injector orifices. The determined scaling factor for the images was 0.3 µm/pixel. A circle was fitted to the orifice using MATLAB. The average diameter of the orifices for the HEUI and CRIN were 154 ± 5.9 µm and 154 ± 1.8 µm, respectively. An observed difference between the orifices on the fuel injectors is that the CRIN orifices are in a plane 90° to the centerline of the injector, whereas, the HEUI orifice plane is slightly canted. A schematic of the layout of the orifices is shown in Figure 5. Figure 6 shows example images, with a circle fitted to the orifice, from the measurements. The lighter color regions on the image of the HEUI injector are due to the light reflecting off of the edge of the orifice. Stock 6-hole injectors were chosen for the experiments described in this paper to provide realistic fuel injection events. Both the HEUI and CRIN injectors retain OEM specifications to preserve the internal flow dynamics of actual injectors on production engines.

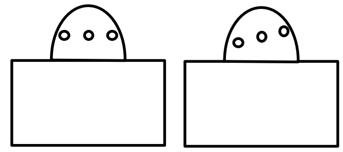

Figure 5. Schematic showing the layout of the orifices on the CRIN (left) and HEUI (right) on the injector tips.

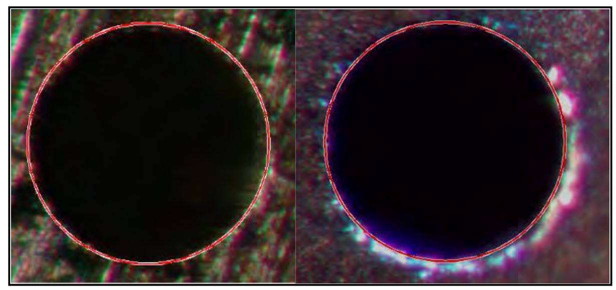

Figure 6. Optical microscopy images of an orifice on the CRIN (left) and HEUI (right) fuel injector.

Figure 7 shows the various plume angles of the HEUI injector. To determine the liquid penetration length, an angle correction must be applied to the measured length. The HEUI injectors investigated are found on a Caterpillar C7 engine and they are installed at an angle in the cylinder head. To direct the fuel toward the piston, the nozzle holes are canted as mentioned earlier and the angle of the plume relative to a vertical plane is shown in Figure 7. To measure the angle, the injector was placed in the injector holder and the angle of the plume to be measured was placed in a vertical direction. Fuel was injected and an image was recorded of the spray event. This process was repeated for all 6 orifices. In addition, the angle was measured for the sprays from the CRIN injector. However, the angle is the same for all the plumes, and was measured to be 10°.

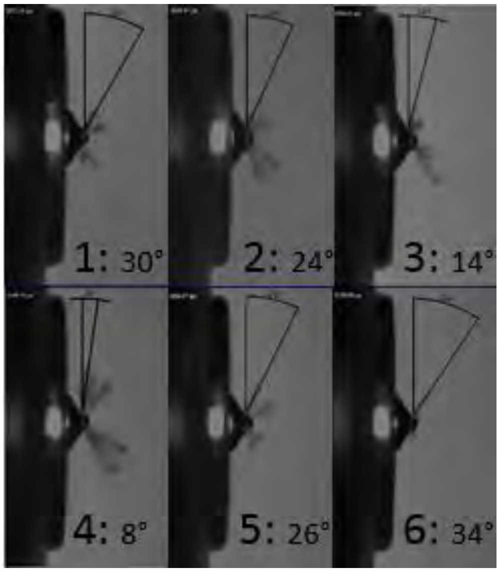

Figure 7. Various measured angles on the HEUI injector. Numbers represent plume orientation convention followed by angle measurement.

Optical Diagnostics and Image Processing

High-speed Mie scattering optical diagnostics were used to characterize the non-reacting fuel spray. A Photron FASTCAM SA-X2 high speed camera, operating at a frame rate of 90,000 fps, coupled to a 100 mm Zeiss Makro-Planar f/2 prime lens was used to acquire the experimental images. Timing of the camera system to a fuel injection event was achieved by using a synchronized output trigger signal from the Drivven injector driver system. The light source used during the experiments consisted of a 632 nm 24 LED array. Light from the array was directed orthogonal to the camera lens and was positioned to provide maximum continuous scattered light. A schematic of the Mie scattering diagnostic setup is shown in Figure 2. With this optical setup, the image size was 384 x 296 pixels and the corresponding scaling factor was 0.153 mm/pixel. The injector holder assembly was rotated to align a vertical spray plume from each fuel injector. LaVison DaVis imaging software was used to process the raw images and determine the spray characteristics. Background subtraction of the raw images to remove undesirable reflected light was conducted and a thresholding technique was applied to determine fuel spray boundaries. A processed image of the CRIN injector highlighting the plume numbering convention is shown in Figure 8, which are consistent with the plume numbers in Figure 7.

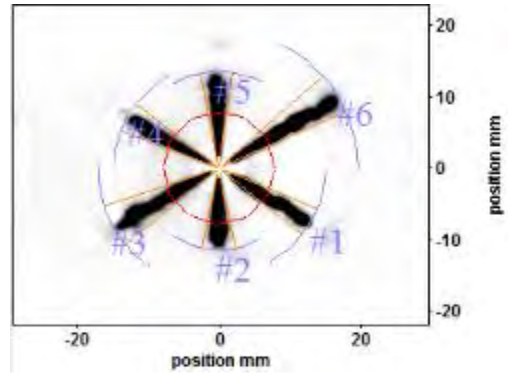

Figure 8. Processed image of CRIN at 1200 bar fuel pressure.

Results and Discussion

The results of the experiments are divided into two sections. First, the results from characterizing the fuel injectors with the ROI instrument will be discussed, followed by the non-reacting spray results obtained with the constant pressure flow chamber.

ROI Experiments

Experiments were performed with a constant injector command for fuel injection pressures of 1080 bar and 1200 bar at 2 different oil temperatures consisting of 45°C and 90°C. Injected fuel mass results (100 shot average) from varying the oil temperature supplied to the HEUI injector are shown in Figure 9. As shown in Figure 9, as the temperature is increased, the injected fuel mass also increases. For the 1200 bar and 1080 bar fuel pressure the injected fuel mass increased by 21% and 30%, respectively. Clearly, there is a dependence on oil temperature and care must be taken during HEUI experiments to control the oil supply temperature. For engine applications operating in cold environments, injector maps must be adjusted to correct for the higher viscosity of the oil [1]. Additional experiments were conducted at various dwell times for the different oil temperatures and results showed similar behavior.

To explore the effects of dwell time on injected fuel mass, HEUI experiments were conducted at a constant oil temperature of 90°C but varying dwell time of the solenoid injector command for fuel pressures of 1080 bar and 1200 bar. Results of the 100 shot average injected fuel mass are shown in Figure 10. As mentioned, dwell time is the time duration between the end of the pilot solenoid current command and the start of the main solenoid current command. Four different dwell times were investigated ranging from 400 us to 900 us. As shown in Figure 10, as the dwell time increases, the injected fuel mass also increases in a near linear relationship of the dwell times investigated. Depending on the desired rate shape of the rate of injection profile, a pilot injection is commanded. The pilot is not to inject fuel from the injector, but to prime the HEUI injector for the main injection event. Depending on when the main solenoid current command occurs after this priming stage, the overall injected fuel mass is effected.

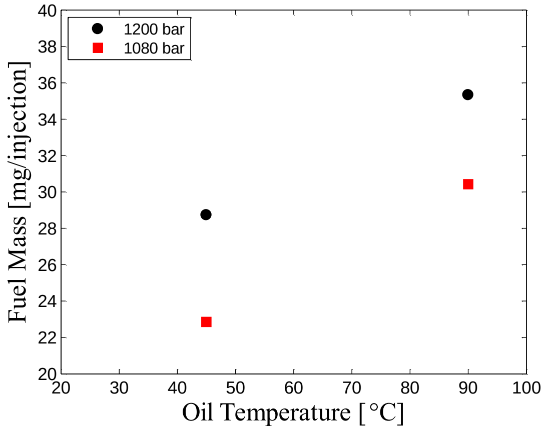

Figure 9. Differences in injected fuel mass from varying oil temperature. Fuel mass is a 100 shot average.

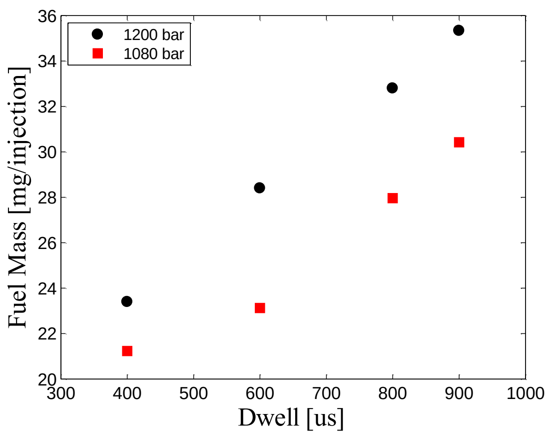

Figure 10. Differences in injected fuel mass from varying dwell time. Fuel mass is a 100 shot average.

HEUI experiments were performed with the ROI instrument to investigate dwell and rate shape effects on ROI behavior. For the experiments, the pilot and main durations were held constant and the oil supply temperature was held at 90°C for each fuel pressure. Results from varying the dwell time of 500 us and 700 us for the 1200 bar fuel pressure case are shown in Figure 11. Injected fuel mass was slightly higher at 14.94 mg for the 700 us dwell case as compared to 14.37 mg for the 500 us dwell. The general shapes of the ROIs are similar, however, for the longer dwell time, the ROI duration is shorter at 650 us compared to 710 us for the 500 us energizing time. In addition, the peak mass flow rate is higher for the 700 us dwell compared to 500 us, with an average of 32.3 mg/ms and 27.9 mg/ms respectively. Similar ROI behavior was observed for the fuel pressures of 850 bar and 1000 bar.

Results from varying the rate shape from 0%, 50%, and 100% for the 1200 bar fuel pressure case are shown in Figure 12. Rate shape percentage is a designation of ROI profile shape, where 100% rate shape results in a sharp increase in penetration rate and a flat top profile. For the rate shape experiments, the injected mass was held constant at approximately 17 mg per injection by varying the current command profile. The current command for the 50% and 100% rate shape cases include a pilot and dwell time, however, for the 0% rate shape only a main duration is commanded. Clearly, rate shapes from the HEUI vary depending on the commanded current profile, as shown in Figure 12. The 100% rate shape shows a sharp rise in initial transient ROI, followed by a plateau region. Whereas, the initial rate is slower for the 50% and 0% rate shape. Depending on the combustion strategy and engine demand, tuning the rate shape profile to yield a slower initial rate can reduce heat release rate and ultimately reduce NO_x emissions [10]. "Boot-like" injection rate shapes have been shown to reduce NO_x as well [11]. However, when short combustion times are required, a square rate shape represented as the 100% rate shape in Figure 12, can be achieved [9].

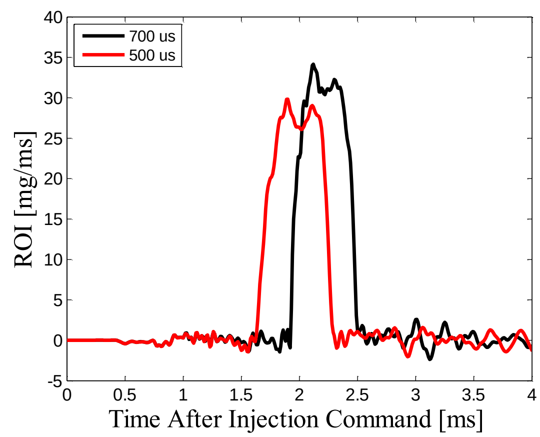

Figure 11. Differences in ROI behavior from varying dwell time for 1200 bar fuel pressure.

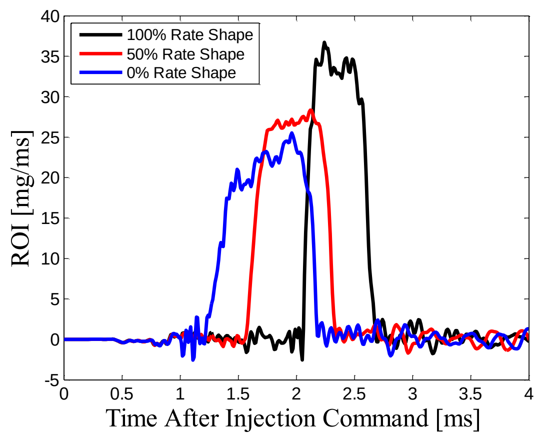

Figure 12. Differences in ROI behavior from varying rate shape for 1200 bar fuel pressure.

To directly compare spray behavior such as liquid penetration length in the constant pressure flow chamber, ROI experiments were conducted to match the rate of injection profiles between the HEUI and CRIN injectors. Experiments were conducted at three different injection pressures consisting of 850, 1000, and 1200 bar fuel pressures. Figure 13 shows the matched ROI profiles for both injectors at a fuel pressure of 850 bar. ROI profiles were first obtained for the CRIN injector and the commanded injection profile for the HEUI was adjusted to match the CRIN. The pilot and dwell times were held constant, and the main injection duration was varied to match the ROIs. For each fuel pressure, the overall injected fuel mass was held constant and below 20 mg for future combustion experiments in the constant pressure flow chamber. For each rail pressure of 850, 1000, 1200 bar the average injected mass was 14.3, 15.8, 18.9 mg, respectively. The time from the start of the current command for the injector to the initial rise in ROI is the hydraulic delay. Comparing the hydraulic delay between the HEUI and the CRIN significant differences are observed. The hydraulic delay for the HEUI is much longer than for the CRIN. For the case presented in Figure 13, the hydraulic delays are 2.02 ms and 0.38 ms for the HEUI and CRIN, respectively. However, for the HEUI, the hydraulic delay has a dependence on the dwell time. A longer dwell time will increase the hydraulic delay. To isolate the dwell time from affecting the hydraulic delay, a 0% rate shape, which does not have a pilot command, was investigated to determine a minimum hydraulic delay. For a fuel pressure of 850 bar at a 0% rate shape, the hydraulic delay was reduced to 1.3 ms. The minimum injector solenoid energizing time for fuel injection from the HEUI without a pilot was found to be 1 ms. No injected fuel was measured for time durations less than 1 ms. Similar trends in ROIs and hydraulic delays were obtained for 1000 and 1200 bar fuel pressures. However, for higher fuel pressures the hydraulic delay was reduced, decreasing to 1.2 ms for the 1200 bar fuel pressure case.

Figures 14 and 15 show the shot-to-shot variability in injected fuel mass between the HEUI and CRIN injectors, respectively, for all three fuel pressures. The ROI profiles were held constant between the HEUI and CRIN for each fuel pressure examined. Overall, similar deviations in injected fuel mass were present for each injector over the range of fuel injection pressures. However, the HEUI shows more fluctuations in shot-to-shot injected fuel mass when compared to the CRIN injector. The average standard deviation of all fuel pressures is 0.69 mg and 0.16 mg for the HEUI and CRIN, respectively. Therefore, the CRIN injector shows approximately 4 times more precise control of injected fuel mass than the HEUI.

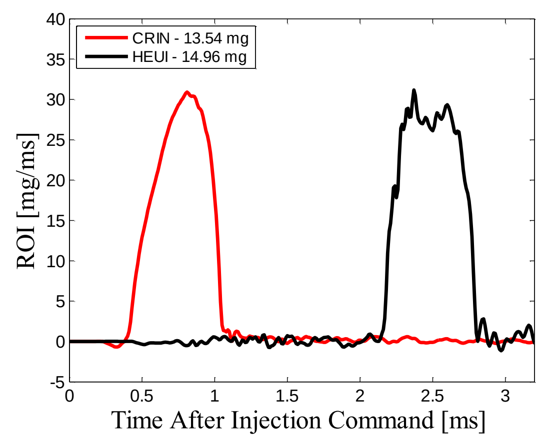

Figure 13. Average ROI profiles for both the HEUI and CRIN at 850 bar fuel pressure.

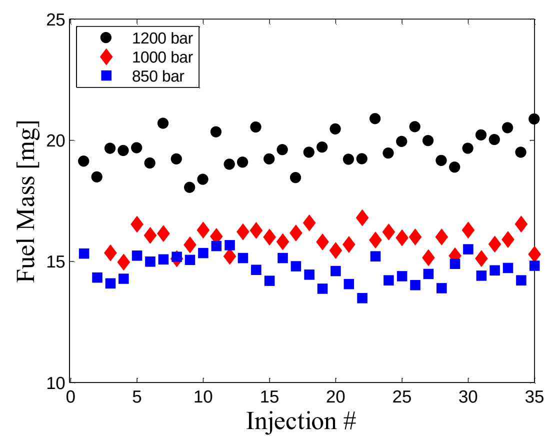

Figure 14. Shot-to-to variability for the HEUI.

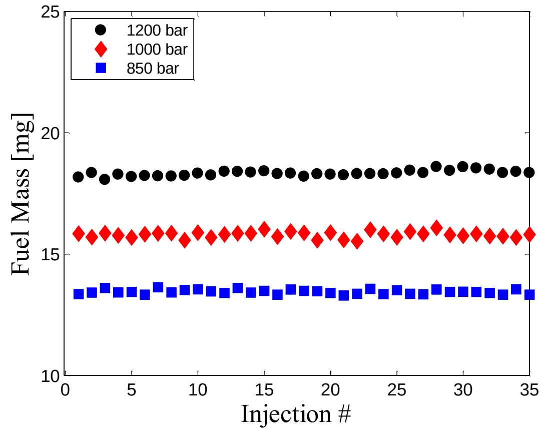

Figure 15. Shot-to-to variability for the CRIN.

Non-Reacting Spray Experiments

Figure 16 shows the processed Mie scattering images for both the CRIN and HEUI for the 1200 bar fuel pressure experiment. Conventional unprocessed Mie scattering images of liquid sprays will appear bright on a dark background in color. However, for image quality and presentation the pixel values during image processing were inverted, thus leading to a dark liquid plume. Caution must be taken when visually comparing spray plumes from these image sets. The spray angles for the HEUI can be as large as 34° for plume 6 thus making the plume to appear much shorter in this two-dimensional representation of the spray events. However, the general spray trends can be observed. The spray plumes from the CRIN injector can directly be compared to one another since the angles are the same at 10°. In addition, starting at the timestamp of 55.56 us for the HEUI images, it appears that the spray from plume 3 starts farther away from the center of the injector than the other plumes. However, during image processing, background subtraction was performed to remove undesirable effects from reflected light. In this small region, light was being scattered off the injector holder and during background subtraction the intensity level in this region goes to zero, thus showing a white area directly in the spray plume. Nevertheless, the tip of the spray is clearly observed. For direct comparison of image sequences, the timestamp on the images is referenced to the time after fuel is injected from the nozzle. As shown earlier, hydraulic delay is much longer for the HEUI than the CRIN. Therefore, actual image time is much longer for the HEUI relative to the start of injection command. During the initial transient region, the spray plumes appear to be relatively consistent. However, as the spray plume develops fluctuations are present in the sprays. These fluctuations are observed for both the CRIN and HEUI injectors. Plume to plume differences have also been observed in a study with an 8-hole common rail injector [12]. It has been hypothesized that the fluctuations are due to temperature gradients caused by fuel evaporation and turbulent eddies near the tip [13]. As the plumes reach a quasi-steady liquid penetration length, the tip of the plume appears to detach from the main jet. This behavior is shown in the 311.11 us case for plume 6 of the CRIN injector. The mentioned behavior is also observed from other HEUI images not shown in this sequence. Similar qualitative spray behavior is observed between injectors for both the 1000 and 850 bar fuel pressure cases.

Select time sequence images, where the time is relative to the start of fuel injection, of different pressures are shown in Figure 17. For each pressure, images at times 88.89 us and 311.11 us are presented to highlight pressure effects on spray plume behavior. Similar observations are observed as discussed earlier. Differences in liquid penetration length and plume to plume fluctuations are present for all fuel pressures. In addition, decreasing the fuel injection pressure will lower the injection velocity, thus slowing the fuel penetration rate. This can be observed as a slight decrease in penetration length during the transient regime of the spray formation. Also observed in the 850 bar case for the HEUI is a difference in liquid length. At the time of 88.89 us after fuel injection, the liquid length is much shorter compared to that of the CRIN indicating variations in hydraulic delay. Overall, differences are observed in spray plume behavior at all pressures examined.

Figure 18 shows liquid penetration plume-to-plume comparison results for each injector type at the various fuel pressures studied. The liquid penetration lengths have been corrected for the angle of the spray. The plots for each injector show the average penetration length of ten fuel injection events for each spray plume. During early transient spray penetration for the CRIN, liquid length is relatively consistent between each plume on the injector and the start of injection occurs near 0.3 ms for both 1200 bar and 850 bar fuel pressures and slightly earlier for the 1000 bar case. As the spray plume increases in liquid length and approaches the quasi-steady regime, larger plume to plume differences are observed. The HEUI injection behavior is much different than the CRIN. The average hydraulic delay is longer for the higher fuel pressures and an increase in variability in start of injection from each plume is present. This observation is also shown in the spray image in Figure 17 at a time of 88.89 us for the 850 bar fuel injection pressure case for the HEUI. As mentioned earlier, as the spray approaches the quasi-steady liquid length regime, the tip can become detached from the main fuel jet. Plume 5 for the HEUI at a pressure of 100 bar quantifies this observation as a sudden decrease in liquid length near 2.4 ms after injection command. The general trend observed is that the HEUI shows more variations in plume to plume transient liquid penetration length than the CRIN injector. To emphasize the difference in start of

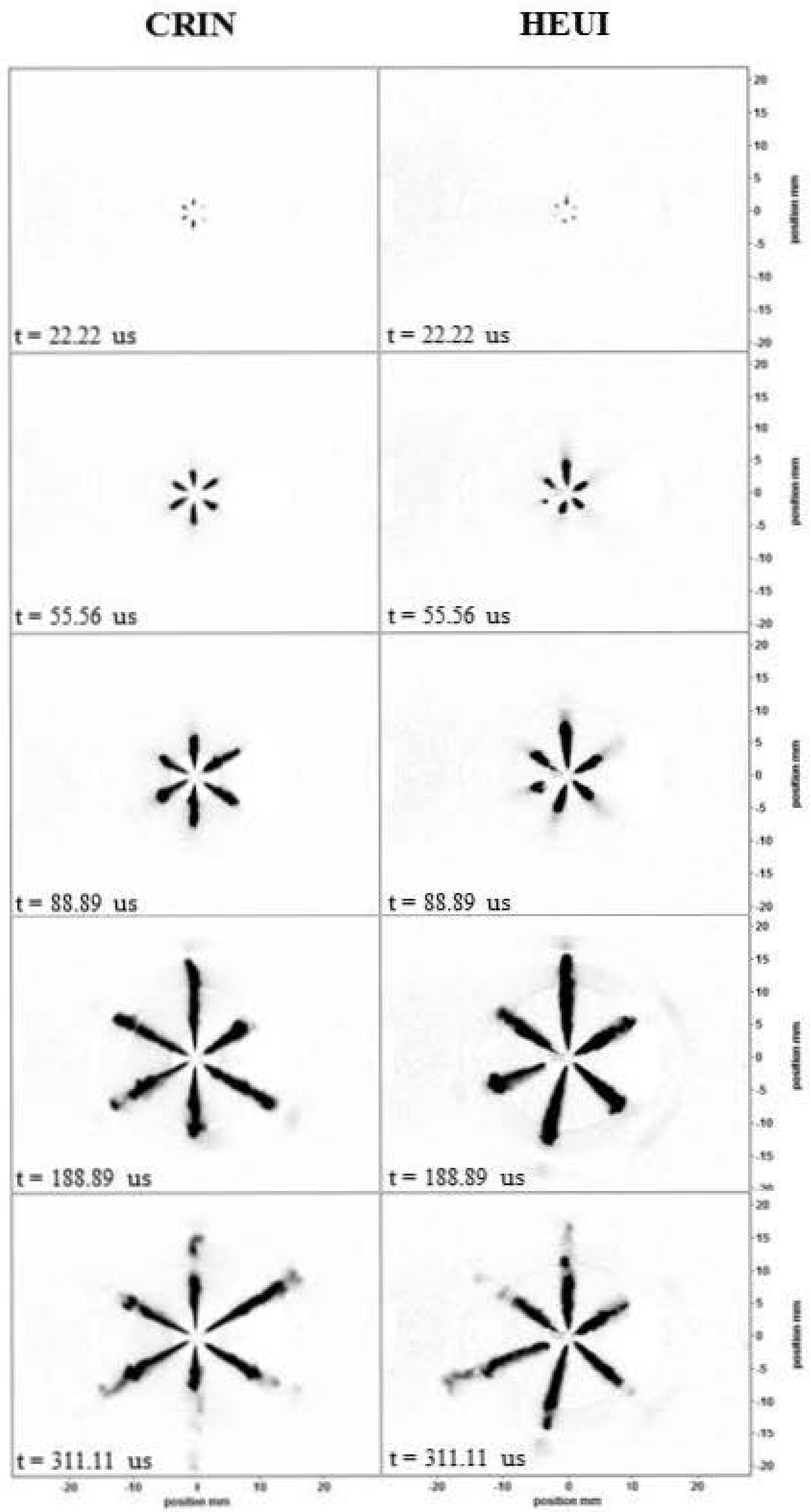

Figure 16. Comparison of time sequence, after start of fuel injection, Mie images for the CRIN and HEUI at 1200 bar fuel pressure.

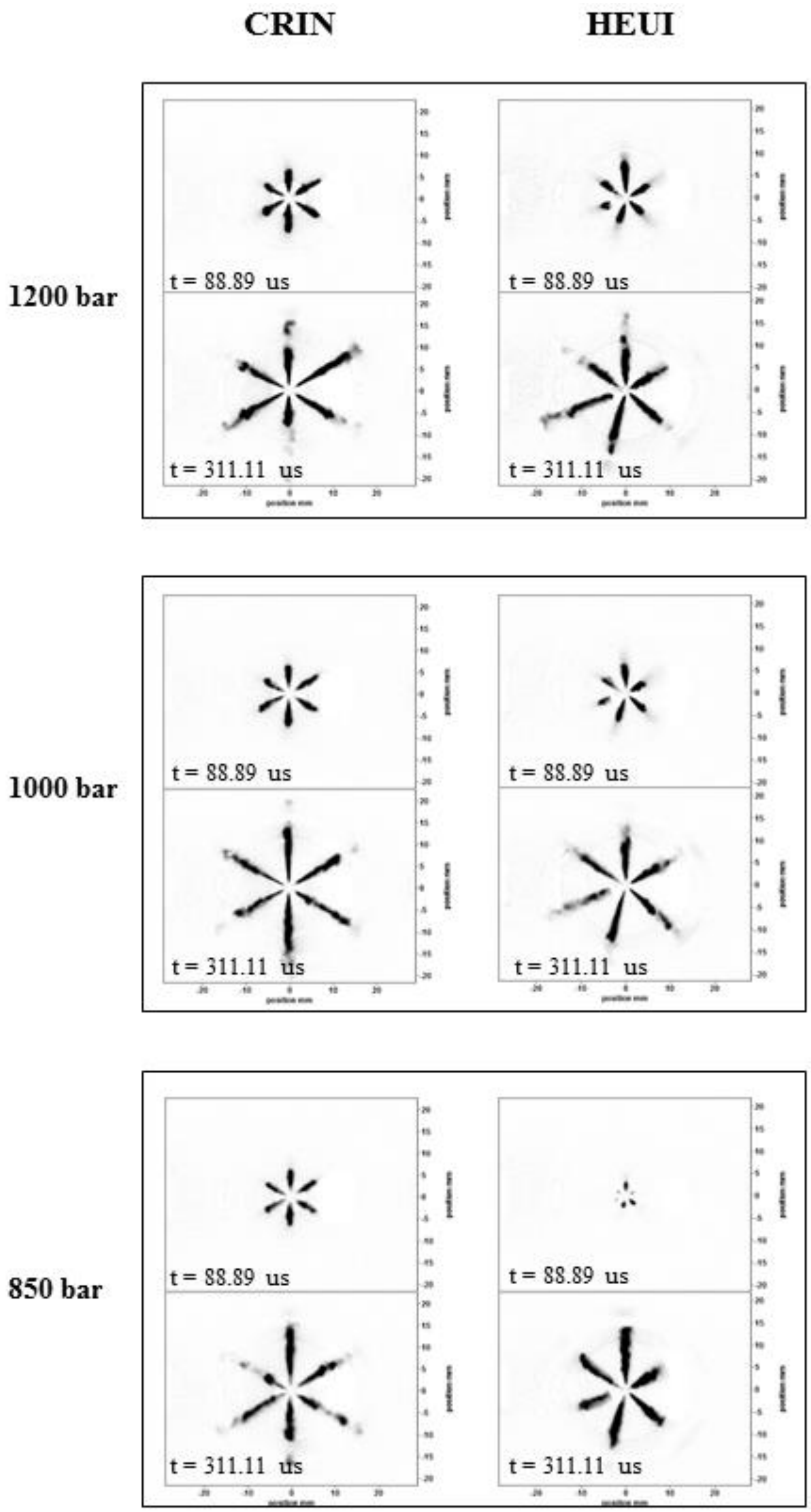

Figure 17. Comparison of select time sequence, after start of fuel injection, Mie images for the CRIN and HEUI at 1200, 1000, 850 bar fuel pressure.

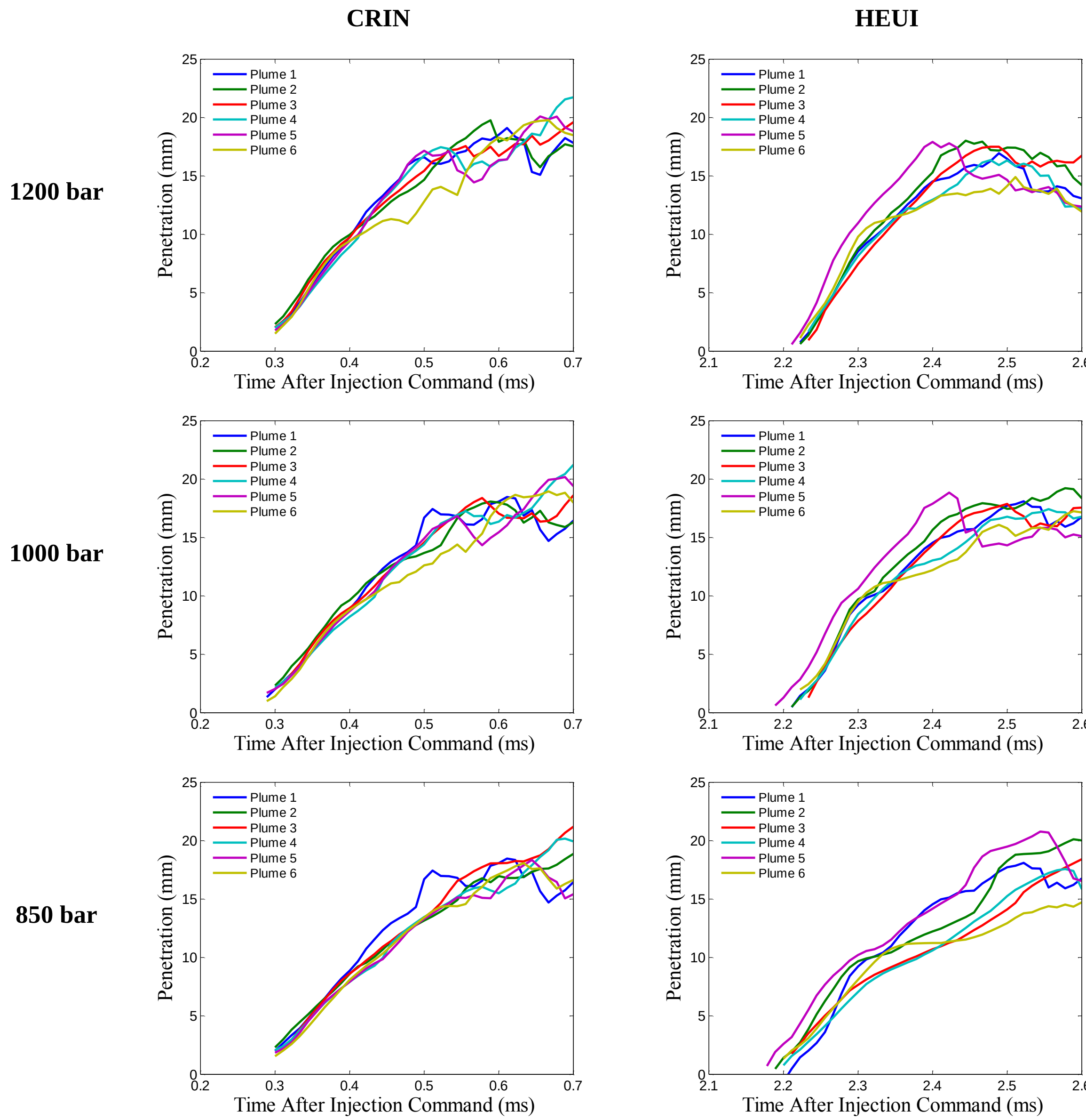

Figure 18. Comparison of average plume-to-plume liquid penetration for the CRIN and HEUI injectors at 1200 bar, 1000 bar, and 850 bar fuel pressures.

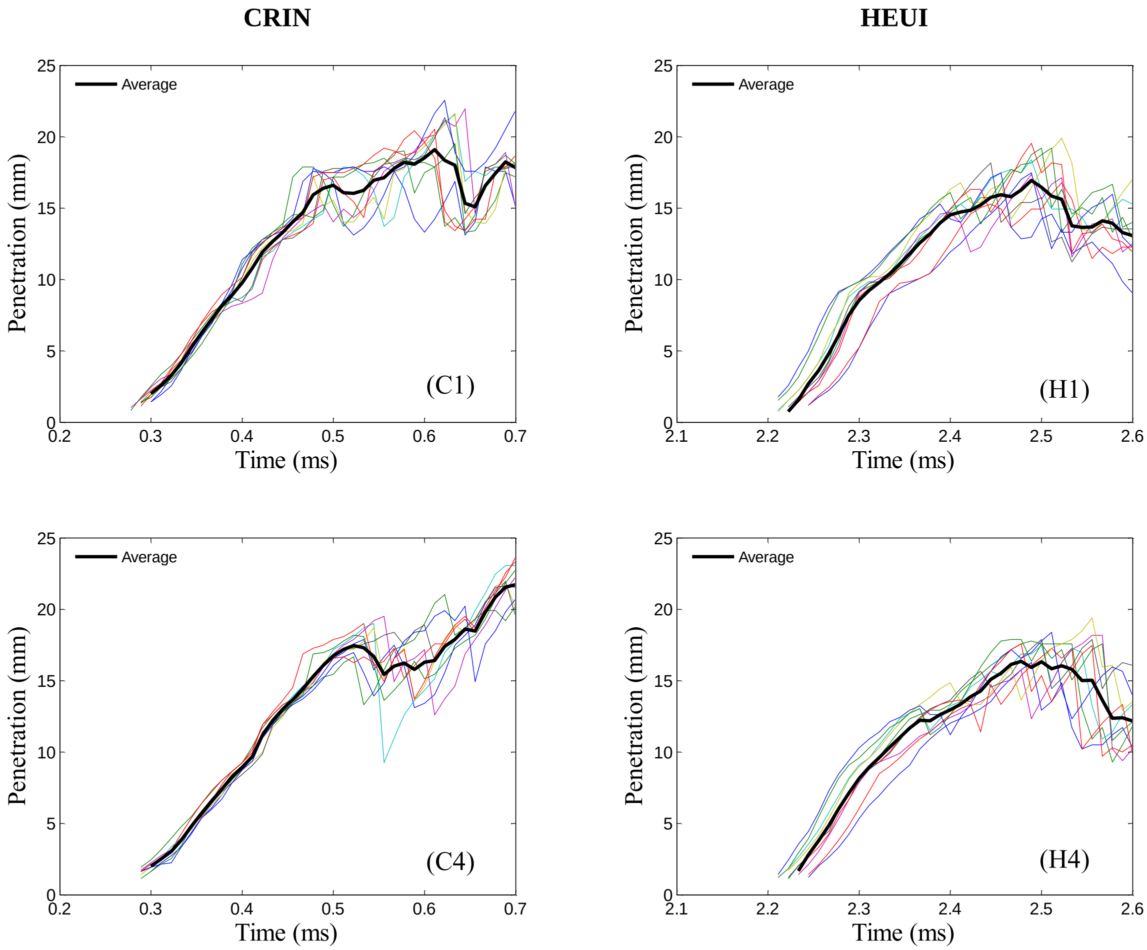

Figure 19. Comparison of plume 1 and plume 4 of the CRIN and HEUI injector at 1200 bar fuel pressure. Each plot shows the penetration length of 10 experiments at the same conditions in addition to the average liquid penetration length.

injection, Figure 19 shows each of the ten spray plume liquid length measurements plus the average, for plume 1 and 4 for each injector at 1200 bar fuel pressure. From the plots, it is evident that the HEUI shows much more variability in the start of fuel injection than the CRIN. The variability is consistent between all six spray plumes of the HEUI.

A comparison of select spray plumes 3, 4, and 5 at all three fuel pressures with 95% confidence limits are shown in Figure 20. Plumes 4 and 5 of the CRIN show that as the pressure increases the transient penetration rate also increases. However, for the HEUI, the transient penetration behavior tends to overlap for the 1200 bar and 1000 bar fuel injection cases indicating that the penetration rate is the same. Further experiments varying injection pressure and an in-depth analysis will need to be conducted to confirm this behavior. The transient penetration rate behavior for the HEUI 850 bar case is lower than both rates for the 1200 bar and 1000 bar fuel pressures. For both injectors, a decrease is observed in penetration length as the spray reaches the quasi-steady regime. In addition, an increase in standard deviation is observed near the start of the regime. Another observation is that the start of injection for the CRIN is consistent at approximately 0.3 ms whereas variations are observed with the HEUI. Injection pressure shows an effect on start of injection with earlier injection for lower fuel pressures.

To directly compare transient liquid penetration length behavior between injectors, the penetration lengths are plotted on the same graph for fuel injection pressures of 1200 bar and 850 bar and the results are shown in Figures 21 and 22, respectively. The penetration length is plotted with respect to the time after start of fuel injection to compare the transient rate. The plume number is indicated in the lower right corner of the plots. The general trend of both injectors is relatively consistent for the 1200 bar fuel injection pressure. However, plume 5 shows a variation of approximately 3 mm in the transient regime. For the lower fuel pressure of 850 bar, larger differences are observed. The CRIN shows a trend of a larger penetration length for all plumes compared to the HEUI except for plume 5 which shows similar behavior. An interesting behavior appears for the HEUI at 850 bar fuel pressure. The transient rate behavior tends to be similar as the CRIN, however, near 0.13 ms the penetration rate decreases. Upon further analysis of the ROI profile for this pressure, as shown in Figure 13, a slight rate shape change is present near 2.3 ms, which is approximately 0.13 ms after start of fuel injection, confirming that the difference in transient penetration length is due to the rate shape profile of the HEUI injector.

Conclusions

Experiments were conducted to investigate and compare JP-8 spray behavior emanating from CRIN and HEUI fuel injectors. ROI experiments were performed to determine the injected fuel mass and rate of injection profiles. CRIN ROI profiles were established as a baseline for fuel pressures consisting of 850 bar, 1000 bar, and 1200 bar. The ROIs and injected fuel mass for the HEUI injector were tuned to match those of the CRIN. Further ROI experiments were conducted with the HEUI to explore oil temperature, rate shape, and dwell effects on injected mass and ROI behavior. In addition, non-reacting JP-8 spray experiments were carried out at realistic engine operating conditions in a constant pressure flow chamber to compare transient liquid penetration behavior between both fuel injector systems. A summary of the results from this study are as follows:

- Oil temperature has a significant effect on injected fuel mass for the HEUI system. An increase of 21% and 30% in injected fuel mass was observed for fuel pressures of 1200 bar and 1080 bar. In addition, increasing the dwell time for the HEUI system, increases injected fuel mass.
- The CRIN injector shows 4 times more precise control of injected fuel mass compared to the HEUI injector.
- More variations in initial start of fuel injection from the HEUI are present compared to that of the CRIN. A lower fuel injection pressure was shown to cause earlier fuel injection for the HEUI. However, no fuel pressure effects on start of injection were observed for the CRIN.
- The plume to plume transient liquid penetration length behavior varies more with the HEUI than the CRIN.
- For matched ROIs, transient liquid penetration length behavior is similar for the 1200 bar fuel pressure between both injectors. Early transient behavior for the 850 bar pressure case is similar between injectors, however, differences in later times are due to HEUI ROI behavior.

Acknowledgements

This research was supported in part by an appointment to the U.S. Army Research Laboratory Postdoctoral Fellowship program administered by Oak Ridge Associated Universities through a contract with the U.S. Army Research Laboratory.

In addition, we would like to acknowledge Dr. Tim Edwards of the Air Force Research Laboratory for supplying the JP-8 and Dr. Chris Gehrke from Caterpillar for technical support.

References

1. Glassey, S.F., Stockner, A.R., Flinn, M.A., *SAE* 930270 (1993).
2. Stockner, A.R., Flinn, M.A., Camplin, F.A., *SAE* 930271 (1993).

3. Mulemane, A., Han, J.-S., Lu, P.-H., Yoon, S.-J., Lai, M.,-C., *SAE* 2004-01-0536 (2004).
4. EL-Hannouny, E.M., Lee, T.W., Farrell, P.V., Reitz, R.D., *SAE* 2003-01-0705 (2003).
5. Fisher, B., and Mueller, C., *SAE International Journal of Engines* 5:415-429 (2012).
6. Ramírez, A.I., Som, S., Aggarwal, S.K., Kastengren, A.L., El-Hannouny, E.M., Longman, D.E., Powell, C.F., *SAE* 2009-01-0846 (2009).
7. Staples, L.R., and Reitz, R. D., *SAE* 2009-01-1124 (2009).
8. Bosch, W., *SAE* 660749 (1966).
9. Coldren, D.R., Schuricht, S.R., Smith III, R.A., *SAE* 2003-01-1384 (2003).
10. Ramírez, A.I., Som, S., Rutter, T.P., Longman, D.E., Aggarwal, S.K., *Spring Technical Meeting of the Central States Section of the Combustion Institute*, Dayton, Ohio, April 2012.
11. Desantes, J.M., Benajes, J., Molina, S., González, C.A., *Applied Thermal Engineering* 24:2701-2714 (2004).
12. Nesbitt, J.E., Naber, J.D., Lee, S.-Y., Kurtz, E., Ge, H.-W., Robarge, N., *23rd Annual Conference on Liquid Atomization and Spray Systems*, Ventura, California, May 2011.
13. Johnson, J., Ge, H.-W., Naber, J., Lee, S.-Y., Kurtz, E., Robarge, N., *SAE International Journal of Engines* 6:1202-1212 (2013).

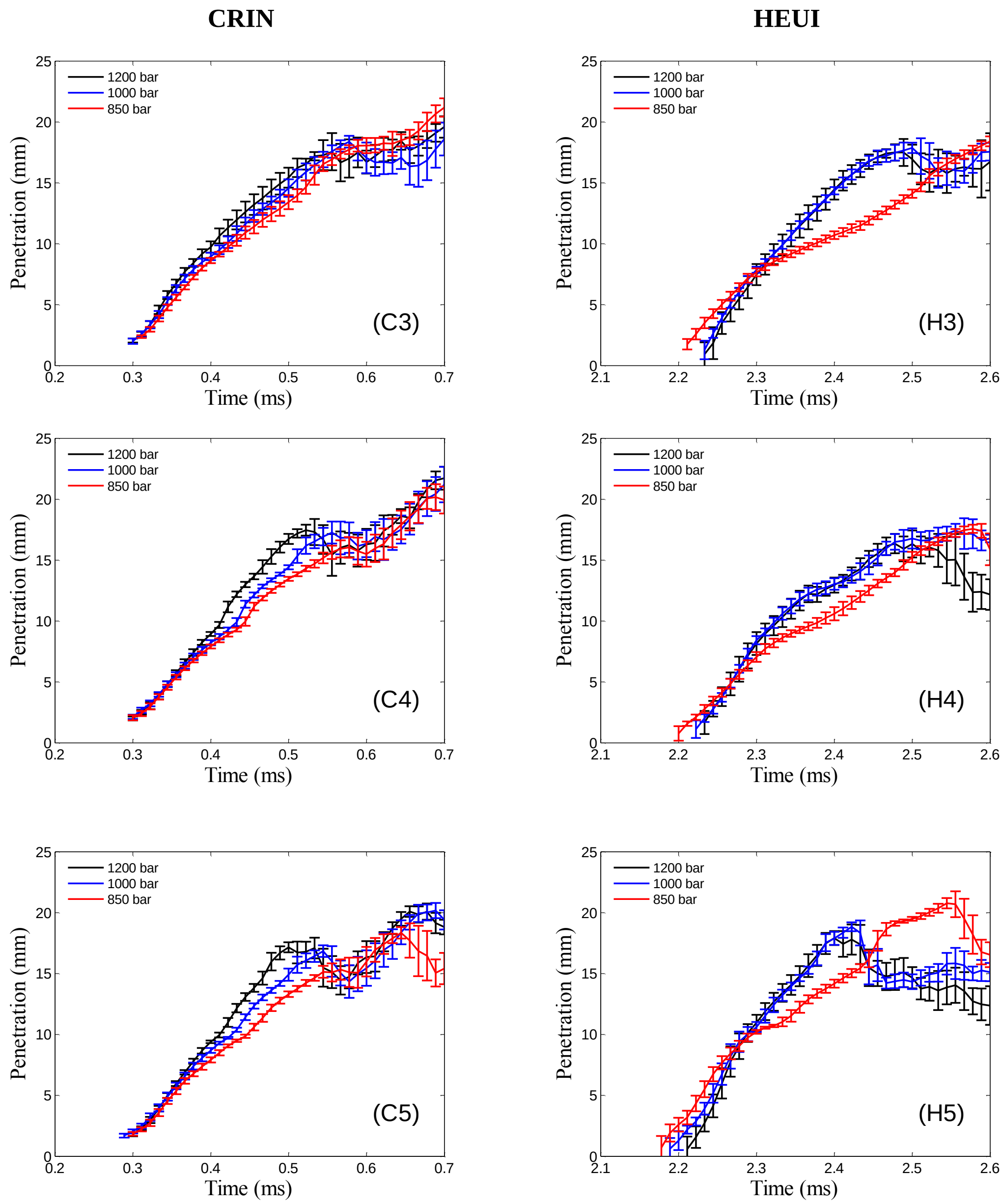

Figure 20. Comparison of liquid penetration length with confidence interval at all pressures for selected plumes 3, 4, and 5 for both the CRIN (labeled C3, C4, and C5) and HEUI (H3, H4, and H5) injectors.

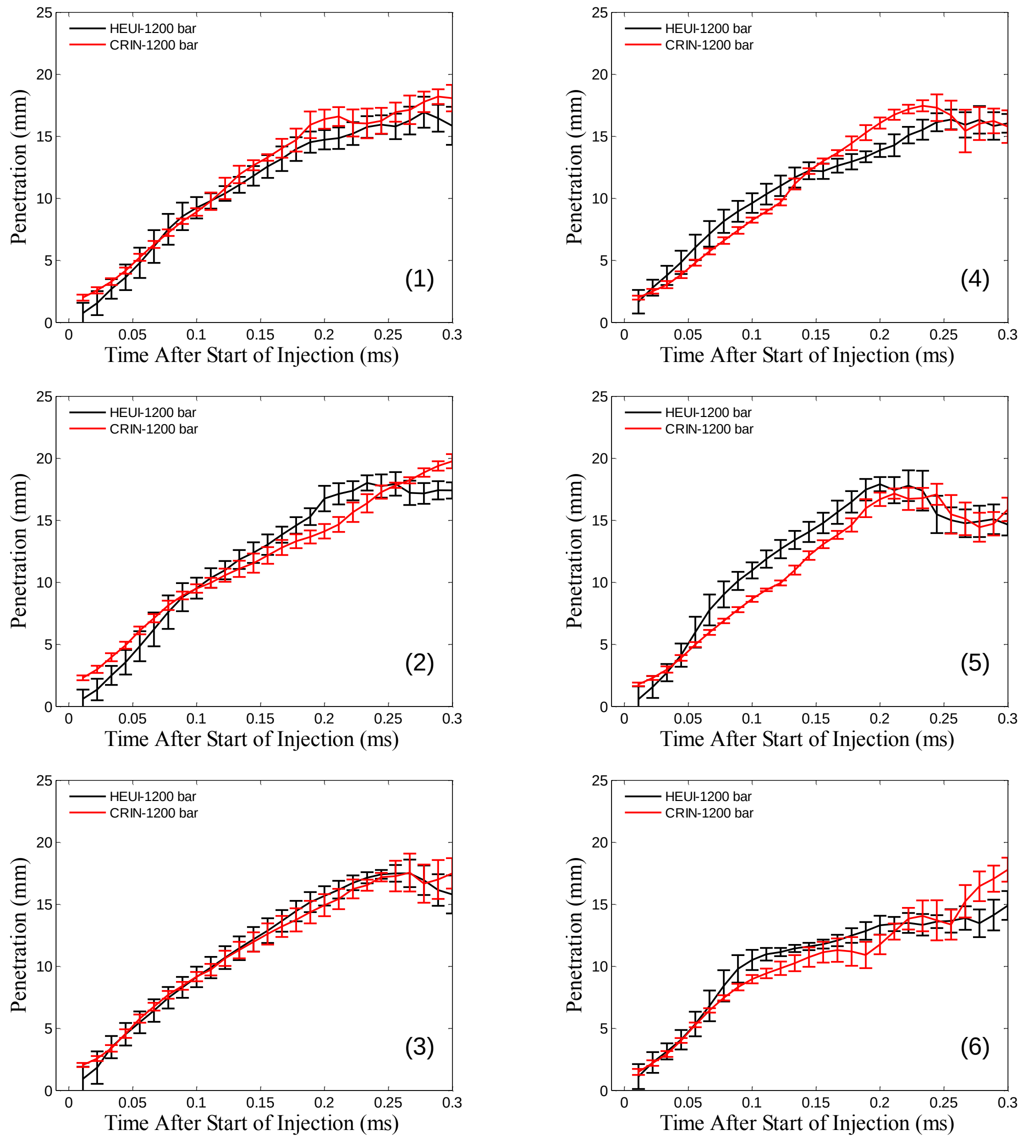

Figure 21. Comparison of transient liquid penetration length between the CRIN and HEUI at 1200 bar fuel pressure. Plume numbers are indicated on each plot.

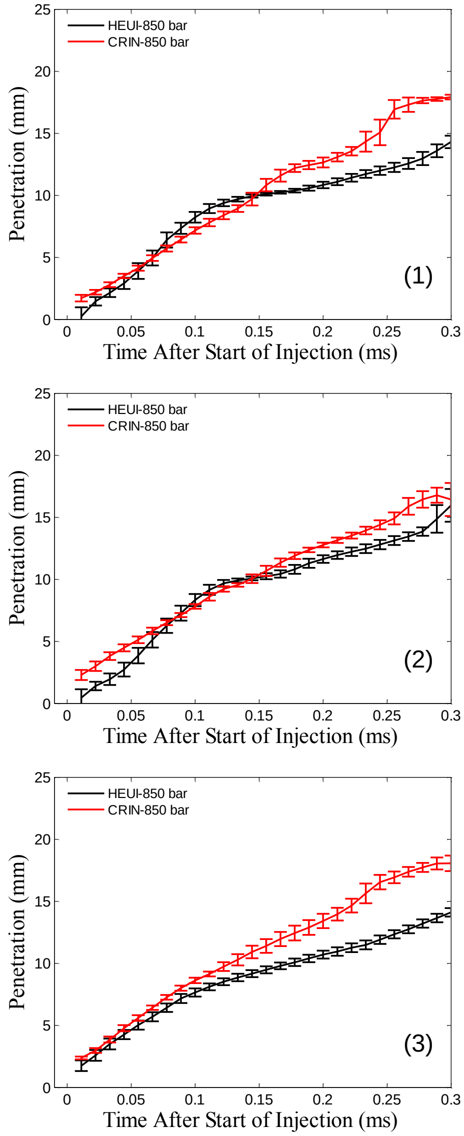

Figure 22. Comparison of transient liquid penetration length between the CRIN and HEUI at 850 bar fuel pressure.

1 (PDF)	DEFENSE TECHNICAL INFORMATION CTR DTIC OCA
2 (PDF)	DIRECTOR US ARMY RESEARCH LAB RDRL CIO LL IMAL HRA MAIL & RECORDS MGMT
1 (PDF)	GOVT PRINTG OFC A MALHOTRA
4 (PDF)	DIR USARL RDRL VTP M KURMAN M TESS L BRAVO C-B KWEON
1 (PDF)	USAMSAA C HERSHEY